Publications of the Korean Astronomical Society
32: 299 ∼ 303, 2017 March

pISSN 1225-1534
eISSN 2287-6936
https://doi.org/10.5303/PKAS.2017.32.1.299

LOCAL ULTRALUMINOUS INFRARED GALAXIES IDENTIFIED IN THE AKARI ALL SKY SURVEY

E. Kilerci Eser[1], T. Goto[2], and Y. Doi[3]

[1]Dark Cosmology Centre, Niels Bohr Institute, University of Copenhagen, Juliane Maries Vej 30, DK-2100 Copenhagen Ø, Denmark
[2]National Tsing Hua University, No. 101, Section 2, Kuang-Fu Road, Hsinchu, Taiwan 30013
[3]The University of Tokyo, Komaba 3-8-1, Meguro, Tokyo, 153-8902, Japan

E-mail: ecekilerci@dark-cosmology.dk

(Received July 31, 2015; Revised October 20, 2016; Accepted October 20, 2016)

ABSTRACT

We crossmatch *AKARI* all-sky survey with the Sloan Digital Sky Survey Data Release 10 (SDSS DR10) and the Final Data Release of the Two-Degree Field Galaxy Redshift Survey (2dFGRS) and identify 118 Ultraluminous Infrared Galaxies (ULIRGs) and one Hyperluminous Infrared Galaxy (HLIRG). We find 40 new ULIRGs and one new HLIRG. ULIRGs in our sample are interacting galaxies or ongoing/post mergers. This is consistent with the fact that ULIRGs are major mergers of disk galaxies. We find that compared to local star forming SDSS galaxies of similar mass, local ULIRGs have lower oxygen abundances and this is consistent with the previous studies.

Key words: astronomy — astrophysics — journals: individual: PKAS

1. INTRODUCTION

Ultraluminous infrared galaxies (ULIRGs) and hyperluminous infrared galaxies (HLIRGs) are defined by their IR luminosities (see the reviews by Sanders & Mirabel, 1996; Lonsdale et al., 2006). ULIRGs have infrared luminosities in the $10^{12}L_{\odot} \leq L_{IR} < 10^{13}L_{\odot}$ range and HLIRGs have infrared luminosities $10^{13}L_{\odot} \leq L_{IR}$. The IR luminosity of these sources is produced by dust that absorbs and re-emits the radiation from star formation and active galactic nuclei (AGN). Local ULIRGs are mostly interacting galaxies and major mergers (Veilleux et al.,, 2002). ULIRGs are considered to be an important phase in the formation of quasars Sanders et al. (1988); Veilleux et al., (2002). In this scenario, during the major merger the molecular gas clouds channel towards the nucleus and trigger nuclear starbursts and the accretion of the matter on to the central super massive black hole (SMBH) starts the AGN activity. The merger evolves to a dust-enshrouded AGN phase, after the gas and dust are consumed the system becomes a bright QSO.

ULIRGs are rare sources in the local (z <0.2) Universe (e.g., Soifer et al., 1987). ULIRGs are more common sources at high redshifts ($z \geq 2$), (e.g., Chapman et al., 2005) and they represent the most rapidly star forming and highly obscured galaxies. High-z ULIRGs and local ULIRGs have different morphological properties, high$-z$ ULIRGs are also non-interacting galaxies (Kartaltepe et al., 2012). Observations show that the properties of ULIRGs change with redshift (e.g Farrah et al., 2008; Takagi et al., 2010; Rujopakarn et al., 2011). Comparison of local and high-z ULIRGs is essential to obtain a complete picture of their evolution across cosmic time. Local ULIRGs are key to study the origin of high IR luminosities and the role of the AGN activity and star formation in nearby mergers. Therefore, local ULIRGa are important.

In this work we identify ULIRGs and HLIRGs in the *AKARI* all-sky survey (Murakami et al., 2007). We cross-correlate *AKARI* all-sky survey with Two-Degree Field Galaxy Redshift Survey (2dFGRS) (Colless et al., 2001) and Sloan Digital Sky Survey (SDSS) DR 10 spectroscopic redshift catalogue (Ahn et al., 2014). We use

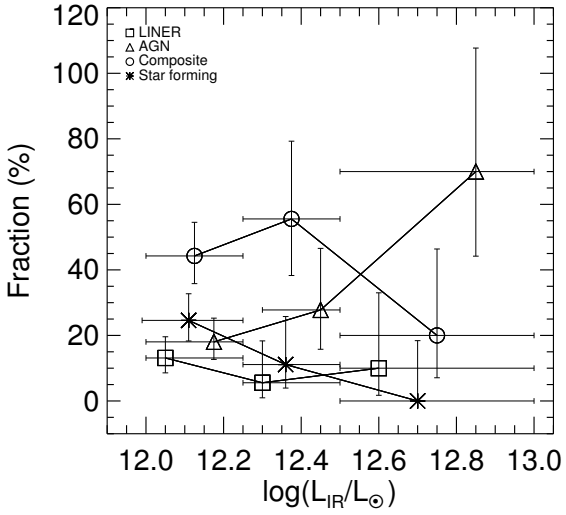

Figure 1. Spectral class fraction versus IR luminosity bins for 89 ULIRGs.

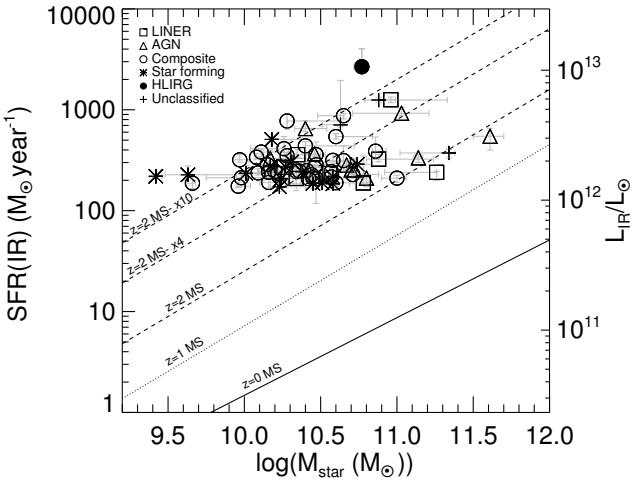

Figure 2. SFR(IR) versus stellar mass for 75 ULIRGs and one HLIRG. The solid line is the z=0 'Main Sequence' of Elbaz et al. (2007). The dotted line is the z=1 'Main Sequence' of Elbaz et al. (2007). The dashed line is the z=2 'Main Sequence' of (Daddi et al., 2007) and the top dashed lines are 4 and 10 times z=2 'Main Sequence'.

the available optical images, spectra, provided by SDSS D10 catalogs and investigate the he morphologies, stellar mass and metallicities of the ULIRGs identified in the *AKARI* all-sky survey.

This paper is organized in the following structure. We introduce our sample in §2. We present our results in §3. We give our conclusions in § 4. In this work, we use a cosmology with $H_0 = 70\,\mathrm{km\,s^{-1}\,Mpc^{-1}}$, $\Omega_\Lambda = 0.7$ and $\Omega_\mathrm{m} = 0.3$.

2. SAMPLE

We cross-match the *AKARI*/IRC all-sky survey point source catalog version 1[1] and the *AKARI*/FIS all-sky survey bright source catalog version 1[2] (Yamamura et al., 2010). This gives us a single *AKARI*/FIS/IRC catalog of 24701 sources with both FIR and mid-IR fluxes.

We cross-correlate the *AKARI*/FIS/IRC catalog with SDSS DR 10 (Ahn et al., 2014) and spectroscopic redshift catalog the Final Data Release of the 2dFGRS , the catalog of *best spectroscopic observations*[3]. We select matching radii as $20''$ and allow each IR source to match only with one optical galaxy.

We perform a SED-fitting using the *LePhare*[4] (Photometric Analysis for Redshift Estimations) code (Arnouts et al., 1999; Ilbert et al., 2006) and estimate the total IR luminosity between 8μm $-$ 1000μm, L_{8-1000}. We use the *AKARI* fluxes with their associated uncertainties adopted from the *AKARI* catalogs. The FIR SED templates of Dale & Helou (2002) are used as the input library.

We select ULIRGs based on the estimated L_{8-1000} luminosity. After checking the optical and IR galaxy match by visual inspection our sample contains 118 ULIRGs and one HLIRG. 40 ULIRGs and one HLIRG are new identifications. We list the properties of the new ULIRGs identified in this work in Table 1. This table contains the *AKARI* name (column 1), redshift (column 2), total IR luminosity, L_{IR}, (column 2).

3. RESULTS

3.1. Redshift Distribution

The redshift distribution of our sample covers $0.050 < z < 0.487$. The median redshift of our sample is $\bar{z} = 0.181$. 104 ULIRGs are in the $0.050 < z \leq 0.270$ range and 14 ULIRGs are in the $0.270 < z < 0.487$ range.

3.2. The Visual Morphologies

We examine SDSS images to investigate the morphological properties of our sample and classify only the galaxies for which SDSS images are available. We use the interaction classification scheme that is described by Veilleux et al., (2002). For the known ULIRGs, we adopt the interaction classifications from Veilleux et al., (2002)

[1] http://www.ir.isas.jaxa.jp/AKARI/Observation/PSC/Public/RN/AKARI-IRC_PSC_V1_RN.pdf.
[2] http://www.ir.isas.jaxa.jp/AKARI/Observation/PSC/Public/RN/AKARI-FIS_BSC_V1_RN.pdf.
[3] http://www2.aao.gov.au/∼TDFgg/.
[4] http://www.cfht.hawaii.edu/∼arnouts/lephare.html.

Table 1
New ULIRGs Identified in the *AKARI* All-Sky Survey

AKARI-FIS-V1 Name	z	$\log(L_{IR}/L_{\odot})$
J2216028+005813	0.210	$12.83^{+0.15}_{-0.14}$
J0859229+473612	0.180	$12.20^{+0.01}_{-0.09}$
J1443444+184950	0.177	$12.21^{+0.01}_{-0.31}$
J0857505+512037	0.366	$12.89^{+0.07}_{-0.02}$
J1106104+023458	0.283	$12.23^{+0.06}_{-0.06}$
J1157412+321316	0.160	$12.14^{+0.01}_{-0.12}$
J1149200-030357	0.162	$12.02^{+0.02}_{-0.04}$
J0126038+022456	0.242	$12.22^{+0.04}_{-0.06}$
J1556089+254358	0.154	$12.03^{+0.01}_{-0.26}$
J0140364+260016	0.321	$12.77^{+0.06}_{-0.02}$
J1257392+080935	0.272	$12.24^{+0.04}_{-0.02}$
J0800007+152319	0.274	$12.14^{+0.00}_{-0.00}$
J0800279+074858	0.173	$12.12^{+0.00}_{-0.09}$
J0834438+334427	0.166	$12.13^{+0.03}_{-0.20}$
J0823089+184234	0.425	$12.57^{+0.43}_{-0.03}$
J1202527+195458	0.132	$12.05^{+0.04}_{-0.02}$
J0912533+192701	0.233	$12.11^{+0.09}_{-0.04}$
J0941010+143622	0.384	$12.75^{+0.01}_{-0.05}$
J1016332+041418	0.266	$12.39^{+0.03}_{-0.05}$
J1401186-021131	0.172	$12.07^{+0.01}_{-0.08}$
J1258241+224113	0.208	$12.07^{+0.05}_{-0.04}$
J1036317+022147	0.050	$12.06^{+0.03}_{-0.04}$
J1050567+185316	0.219	$12.60^{+0.03}_{-0.06}$
J1111177+192259	0.225	$12.60^{+0.03}_{-0.06}$
J1219585+051745	0.487	$12.87^{+0.02}_{-0.04}$
J1414276+605726	0.151	$12.11^{+0.00}_{-0.12}$
J0936293+203638	0.175	$12.01^{+0.04}_{-0.02}$
J1533582+113413	0.337	$12.32^{+0.08}_{-0.08}$
J1348483+181401	0.179	$12.19^{+0.03}_{-0.03}$
J1125319+290316	0.138	$12.27^{+0.01}_{-0.05}$
J1603043+094717	0.152	$12.02^{+0.03}_{-0.03}$
J1639245+303719	0.224	$12.11^{+0.01}_{-0.05}$
J1050288+002806	0.216	$12.38^{+0.13}_{-0.08}$
J0928103+232521	0.197	$12.07^{+0.08}_{-0.04}$
J2344170+053520	0.267	$12.56^{+0.01}_{-0.19}$
J2353152-313234	0.185	$12.04^{+0.00}_{-0.12}$
J1222488-040307	0.181	$12.19^{+0.02}_{-0.04}$
J1419037-034657	0.152	$12.09^{+0.01}_{-0.08}$
J1048019-013017	0.167	$12.09^{+0.07}_{-0.07}$
J1338353-041131	0.175	$12.14^{+0.12}_{-0.22}$

and Hwang et al. (2007). In order to avoid uncertainties in interaction classifications due to the distances, we only consider the sources within $z = 0.27$. We find the faction of binary systems showing strong interaction features as 43%. The fraction of late/post mergers is 52%. This is consistent with the general picture that ULIRGs are interacting galaxies.

3.3. Spectral Classification

To identify the spectral classes of the ULIRGs in our sample we adopt the spectral classification given by Thomas et al. (2013). SDSS spectra are available only for 89 sources. Our sample consists of 19% purely star forming galaxies, 44% composite galaxies, 11% LINERs and 26% AGN.

The fraction of ULIRGs in different spectral classes as a function of IR luminosity is shown in Figure 1. We find that the fraction of AGNs grows with increasing L_{IR}. This trend agrees with the results of previous studies showed a correlation between the AGN fraction and IR luminosity (Veilleux et al., 1995; Kim et al., 1998; Goto, 2005).

3.4. Position of ULIRGs in Star Formation Rate − Stellar Mass Diagram

We adopt the stellar masses (M_{star}) of the ULIRGs in our sample from 'stellarMassPortStarforming'[5] catalog. We compute star formation rate (SFR) based on Eq. (4) given by Kennicutt (1998). We show SFR versus M_{star} for 75 ULIRGs and one HLIRG in Figure 2. The solid line is the 'main sequence' of normal star-forming galaxies (SFGs) at $z \sim 0$ (Elbaz et al., 2007). The dotted line is the $z \sim 1$ 'main sequence' (Elbaz et al., 2007) and the dashed line is the $z \sim 2$ (Daddi et al., 2007) 'main sequence'. The top dashed lines show 4 and 10 times above the $z \sim 2$ 'main sequence' relationship. Local ULIRGs exhibit higher SFRs compared to normal SFGs with the same masses. Compared to the $z \sim 0$, $z \sim 1$ and $z \sim 2$ 'main sequence', on average ULIRGs exhibit 92, 17 and 5 times higher SFRs, respectively. ULIRGs mostly distributed around the dashed line representing 4 times above the $z \sim 2$ MS.

It has been already known that local ULIRGs are outliers compared to the local 'main sequence' (Elbaz et al., 2007). This is expected because, ULIRGs are defined to have SFRs in the range of 172 $\leq$SFR(IR)$\leq$ 1721. Therefore, their position in the SFR axis is a selection effect.

3.5. Position of ULIRGs in Stellar Mass − Gas Metallicity Diagram

We adopt the relevant emission-line fluxes from Thomas et al. (2013) in order to measure the gas metallicity. We compute oxygen abundances, (O/H), by following Eq. (1) of Tremonti et al. (2004). In Figure 3 we show the $M_{star} - Z$ distribution of our sample. We have 48 ULIRGs and one HLIRG for which emission-line fluxes

[5] http://www.sdss3.org/dr10/spectro/galaxy_portsmouth.php.

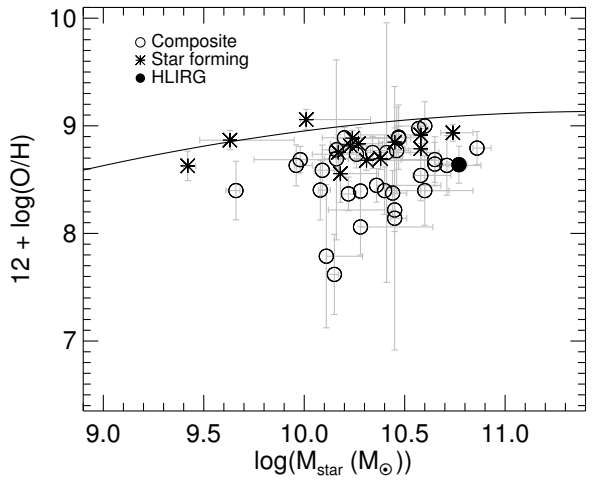

Figure 3. Oxygen abundances versus stellar mass of our sample. The solid is the the mass−metallicity relation of the local SDSS galaxies given by Tremonti et al. (2004).

given by Thomas et al. (2013). The solid line is the $M_{star} - Z$ relationship, Eq. (3) given by Tremonti et al. (2004). Compared to the normal star forming SDSS galaxies with similar masses, local ULIRGs have lower (0.20 dex) oxygen abundances. The lower oxygen abundances of our sample is consistent with the results of Rupke et al. (2008).

4. CONCLUSIONS

We cross-match *AKARI* catalogs with SDSS DR 10 and 2dFGRS and identify ULIRGs in the *AKARI* all-sky survey. We investigate morphologies, stellar masses, SFRs, gas metallicities of local ULIRGs. We examine the positions of ULIRGs in the SFR − M_{star} and $M_{star} - Z$ diagrams. Our main conclusions are:

- Based on the spectroscopic redshifts from SDSS DR10 and 2dFGRS we identify 118 ULIRGs and one HLIRG in the *AKARI* all-sky survey. Among those 40 ULIRGs and one HLIRG are newly identified.
- We investigated interaction classes of 100 ULIRGs and find that 43% are two galaxy systems with strong tidal tails, bridges and 52% are ongoing/post mergers. This supports the known picture of ULIRGs as mergers.
- We confirm the known trend of increasing AGN faction with higher IR luminosity.
- Local ULIRGs have higher SFRs compared to 'main sequence' galaxies with similar mass at $z \sim 0$, $z \sim 1$ and $z \sim 2$.
- Local ULIRGs have lower oxygen abundances compared to SDSS galaxies with similar masses.

REFERENCES

Ahn, C. P., et al., 2014, The Tenth Data Release of the Sloan Digital Sky Survey: First Spectroscopic Data from the SDSS-III Apache Point Observatory Galactic Evolution Experiment, ApJS, 211, 17

Arnouts, S., Cristiani, S., Moscardini, L., Matarrese, S.,Lucchin, F., Fontana, A., & Giallongo, E., 1999, Measuring and modelling the redshift evolution of clustering: the Hubble Deep Field North, MNRAS, 310, 540

Chapman, S. C., Blain, A. W., Smail, I., & Ivison, R. J., 2005, A Redshift Survey of the Submillimeter Galaxy Population, ApJ, 622, 772

Colless, M., et al., 2001, The 2dF Galaxy Redshift Survey: spectra and redshifts, MNRAS, 328, 1039

Daddi, E., et al., 2007, Multiwavelength Study of Massive Galaxies at z˜2. I. Star Formation and Galaxy Growth, ApJ, 670, 156

Dale, D. A. & Helou, G., 2002, The Infrared Spectral Energy Distribution of Normal Star-forming Galaxies: Calibration at Far-Infrared and Submillimeter Wavelengths, ApJ, 576, 159

Elbaz, D., et al., 2007, The reversal of the star formation-density relation in the distant universe, A&A, 468, 33

Farrah, D., et al., 2008, The Nature of Star Formation in Distant Ultraluminous Infrared Galaxies Selected in a Remarkably Narrow Redshift Range, ApJ, 677, 957

Goto, T., 2005, Optical properties of 4248 IRAS galaxies, MNRAS, 360, 322

Hwang, H. S., Serjeant, S., Lee, M. G., Lee, K. H., & White, G. J., 2007, The ultraluminous and hyperluminous infrared galaxies in the Sloan Digital Sky Survey, 2dF Galaxy Redshift Survey and 6dF Galaxy Survey, MNRAS, 375, 115

Ilbert, O., et al., 2006, Accurate photometric redshifts for the CFHT legacy survey calibrated using the VIMOS VLT deep survey, A&A, 457, 841

Kartaltepe, J. S., et al., 2012, GOODS-Herschel and CANDELS: The Morphologies of Ultraluminous Infrared Galaxies at z ˜ 2, ApJ, 757, 23

Kennicutt, Jr., R. C., 1998, Star Formation in Galaxies Along the Hubble Sequence, ARA&A, 36, 189

Kim, D.-C., Veilleux, S., & Sanders, D. B., 1998, The IRAS 1 Jy Sample of Ultraluminous Infrared Galaxies. II. Optical Spectroscopy, ApJ, 508, 627

Lonsdale, C. J., Farrah, D., & Smith, H. E., 2006, Ultraluminous Infrared Galaxies, in Astrophysics Update 2, ed. J. W. Mason (Heidelberg: Springer), 285

Murakami, H., et al., 2007, The Infrared Astronomical Mission AKARI, PASJ, 59, 369

Rujopakarn, W., Rieke, G. H., Eisenstein, D. J., & Juneau, S., 2011, Morphology and Size Differences Between Local and High-redshift Luminous Infrared Galaxies, ApJ, 726, 93

Rupke, D. S. N., Veilleux, S., & Baker, A. J., 2008, The Oxygen Abundances of Luminous and Ultraluminous Infrared Galaxies, ApJ, 674, 172

Sanders, D. B., & Mirabel, I. F., 1996, Luminous Infrared Galaxies, ARA&A, 34, 749

Sanders, D. B., Soifer, B. T., Elias, J. H., Neugebauer, G., & Matthews, K., 1988, Warm ultraluminous galaxies in the IRAS survey - The transition from galaxy to quasar?, ApJ, 328, L35

Soifer, B. T., et al., 1987, The IRAS bright galaxy sample. II - The sample and luminosity function, ApJ, 320, 238

Takagi, T., et al., 2010, Polycyclic aromatic hydrocarbon (PAH) luminous galaxies at z ˜ 1, A&A, 514, A5

Thomas, D., et al., 2013, Stellar velocity dispersions and emission line properties of SDSS-III/BOSS galaxies, MNRAS, 431, 1383

Tremonti, C. A., et al., 2004, The Origin of the Mass-Metallicity Relation: Insights from 53,000 Star-forming Galaxies in the Sloan Digital Sky Survey, ApJ, 613, 898

Veilleux, S., Kim, D.-C. & Sanders, D. B., 2002, Optical and Near-Infrared Imaging of the IRAS 1 Jy Sample of Ultraluminous Infrared Galaxies. II. The Analysis, ApJS, 143, 315

Veilleux, S., Kim, D. -C., Sanders, D. B., Mazzarella, J. M., & Soifer, B. T., 1995, Optical Spectroscopy of Luminous Infrared Galaxies. II. Analysis of the Nuclear and Long-Slit Data, ApJS, 98, 171

Yamamura, I., et al., 2010, VizieR Online Data Catalog: AKARI/FIS All-Sky Survey Point Source Catalogues (ISAS/JAXA, 2010), yCat, 2298, 0